J|A|C|S ARTICLES

Published on Web 09/02/2010

Synthesis, Electronic Structure, and Reactivity of Strained Nickel-, Palladium-, and Platinum-Bridged [1]Ferrocenophanes

Inmaculada Matas,[†] George R. Whittell,[†] Benjamin M. Partridge,[†] Jason P. Holland,[‡] Mairi F. Haddow,[†] Jennifer C. Green,*[,‡] and Ian Manners*[,†]

School of Chemistry, University of Bristol, Cantock's Close, Bristol BS8 1TS, U.K. and Chemistry Research Laboratory, Department of Chemistry, University of Oxford, 12 Mansfield Road, Oxford OX1 3TA, U.K.

Received April 28, 2010; E-mail: jennifer.green@chem.ox.ac.uk; ian.manners@bristol.ac.uk

Abstract: The group 10 *bis*(phosphine)metalla[1]ferrocenophanes, [{Fe(η^5-C_5H_4)$_2$}M(P*n*-Bu$_3$)$_2$] [M = Ni (**4a**), Pd (**4b**), and Pt (**4c**)], have been prepared by the reaction of Li$_2$[Fe(η^5-C_5H_4)$_2$]·tmeda (**5**, tmeda = *N*,*N*′,*N*′-tetramethylethylenediamine) with *trans*-[MCl$_2$(P*n*-Bu$_3$)$_2$] [M = Ni (*trans*-**6a**) and Pd (*trans*-**6b**)] and *cis*-[PtCl$_2$(P*n*-Bu$_3$)$_2$] (*cis*-**6c**), respectively. Single crystal X-ray diffraction revealed highly tilted, strained structures as characterized by α angles of 28.4° (**4a**), 24.5° (**4b**), and 25.2° (**4c**) and a distorted square planar environment for the group 10 metal center. UV/visible spectroscopy and cyclic voltammetry indicated that all three compounds had smaller HOMO−LUMO gaps and were more electron-rich in nature than ferrocene and other comparable [1]ferrocenophanes. DFT calculations suggested that these differences were principally due to the electron-releasing nature of the M(P*n*-Bu$_3$)$_2$ metal−ligand fragments. Attempts to induce thermal or anionic ring-opening polymerization of **4a**−**c** were unsuccessful and were complicated by, for example, competing ligand dissociation processes or unfavorable chain propagation. In contrast, these species all reacted rapidly with acids effecting clean extrusion of the *bis*(phosphine)metal fragment. Carbon monoxide inserted cleanly into one of the palladium−carbon bonds of **4b** to afford the ring-expanded, acylated product [{Fe(η^5-C_5H_4)(η^5-C_5H_4)(CO)}Pd(P*n*-Bu$_3$)$_2$] (**10**). The nickel analogue **4a**, however, afforded [Ni(CO)$_2$(P*n*-Bu$_3$)$_2$] whereas the platinum-bridged complex **4c** was inert. Remarkably, all compounds **4a**−**c** were readily oxidized by elemental sulfur to afford the [5,5′]bicyclopentadienylidene (pentafulvalene) complexes [{η^4:η^0-C_5H_4(C_5H_4)}M(P*n*-Bu$_3$)$_2$] [M = Ni (**11a**)] and [(η^2-$C_{10}H_8$)M(P*n*-Bu$_3$)$_2$] [M = Pd (**11b**) and Pt (**11c**)] by a formal 4-electron oxidation of the carbocyclic ligands. Compounds **11b** and **11c** represent the first examples of [5,5′]bicyclopentadienylidene as a neutral η^2-ligand. The relative energies of η^2-coordination with respect to that of η^4:η^0 bonding were investigated for **11a**−**c** by DFT calculations.

1. Introduction

Strained metallocenophanes and related organometallic rings containing π-hydrocarbon ligands have received much attention due to their interesting structures, bonding, and enhanced reactivity, especially with respect to their role as monomers in ring-opening polymerization (ROP) reactions.[1−3] ROP of a range of these strained metallorings has now been achieved, and this provides a convenient route to high molecular weight metal-containing polymers with a series of potential applications as functional materials.[1−5] To date, the most extensively studied system involves strained sila[1]ferrocenophanes (**1**, ER$_x$ =

[†] University of Bristol.
[‡] University of Oxford.

(1) For a recent review see: Herbert, D. E.; Mayer, U. F. J.; Manners, I. *Angew. Chem., Int. Ed.* **2007**, *46*, 5060.

(2) For examples of [1]ferrocenophanes, see: (a) Osborne, A. G.; Whiteley, R. H.; Meads, R. E. *J. Organomet. Chem.* **1980**, *193*, 345. (b) Foucher, D. A.; Manners, I. *Makromol. Chem. Rapid Commun.* **1993**, *14*, 63. (c) Pudelski, J. K.; Gates, D. P.; Rulkens, R.; Lough, A. J.; Manners, I. *Angew. Chem., Int. Ed. Engl.* **1995**, *34*, 1506. (d) Rulkens, R.; Lough, A. J.; Manners, I. *Angew. Chem., Int. Ed. Engl.* **1996**, *35*, 1805. (e) Sharma, H. K.; Cervantes-Lee, F.; Mahmoud, J. S.; Pannell, K. H. *Organometallics* **1999**, *18*, 399. (f) Schachner, J. A.; Lund, C. L.; Quail, J. W.; Mueller, J. *Organometallics* **2005**, *24*, 4483. (g) Schachner, J. A.; Lund, C. L.; Quail, J. W.; Mueller, J. *Organometallics* **2005**, *24*, 785. (h) Seyferth, D.; Withers, H. P., Jr. *Organometallics* **1982**, *1*, 1275. (i) Sänger, I.; Heilmann, J. B.; Bolte, M.; Lerner, H.-W.; Wagner, M. *Chem. Commun.* **2006**, 2027.

(3) For examples of non-iron metallocenophanes and related species, see: (a) Vogel, U.; Lough, A. J.; Manners, I. *Angew. Chem., Int. Ed.* **2004**, *43*, 3321. (b) Lund, C. L.; Schachner, J. A.; Quail, J. W.; Mueller, J. *Organometallics* **2006**, *25*, 5817. (c) Lund, C. L.; Schachner, J. A.; Quail, J. W.; Mueller, J. *J. Am. Chem. Soc.* **2007**, *129*, 9313. (d) Berenbaum, A.; Manners, I. *Dalton Trans.* **2004**, 2057. (e) Braunschweig, H.; Homberger, M.; Hu, C.; Zheng, X.; Gullo, E.; Clentsmith, G.; Lutz, M. *Organometallics* **2004**, *23*, 1968. (f) Elschenbroich, C.; Schmidt, E.; Gondrum, R.; Metz, B.; Burghaus, O.; Massa, W.; Wocadlo, S. *Organometallics* **1997**, *16*, 4589. (g) Braunschweig, H.; Kupfer, T.; Radacki, K. *Angew. Chem., Int. Ed.* **2007**, *46*, 1630. (h) Tamm, M.; Kunst, A.; Bannenberg, T.; Randoll, S.; Jones, P. G. *Organometallics* **2007**, *26*, 417. (i) Braunschweig, H.; Lutz, M.; Radacki, K.; Schaumlöffel, A.; Seeler, F.; Unkelbach, C. *Organometallics* **2006**, *25*, 4433. (j) Chadha, P.; Dutton, J. L.; Sgro, M. J.; Ragogna, P. J. *Organometallics* **2007**, *26*, 6063. (k) Braunschweig, H.; Kupfer, T. *Acc. Chem. Res.* **2010**, *43*, 455. (l) Sharma, H. K.; Cervantes-Lee, F.; Pannell, K. H. *J. Am. Chem. Soc.* **2004**, *126*, 1326. (m) Tamm, M. *Chem. Commun.* **2008**, 3089.

(4) (a) Archer, R. D. *Inorganic and Organometallic Polymers*; John Wiley & Sons, Inc.: New York, 2001. (b) Whittell, G. R.; Manners, I. *Adv. Mater.* **2007**, *19*, 3439.

(5) Bellas, V.; Rehahn, M. *Angew. Chem., Int. Ed.* **2007**, *46*, 5082.

SiRR′) which are monomeric precursors to polyferrocenylsilanes (**2**, ER_x = SiRR′).[1,4b,5]

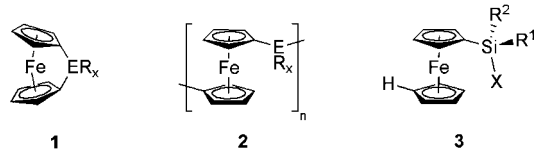

1 **2** **3**

The appreciable ring tilting of the two cyclopentadienyl rings in ferrocenophanes, which can be described by the angles depicted in Figure 1, has been shown to constitute the major contribution to the strain present.[1,5−7] It is this strain that represents the most important thermodynamic factor in determining the propensity of these species to undergo ring-opening reactions. For example, sila[1]ferrocenophanes react readily with protic reagents, such as HCl or MeOH, leading to the cleavage of the Cp−Si bond to yield ring-opened species such as **3** (X = Cl or H).[1,8] Moreover, the kinetic barrier to the ring-opening process can be overcome by thermal, anionic, or catalytic means, thereby enabling the preparation of high molecular weight polyferrocenylsilanes via versatile routes.[1,5,9−11]

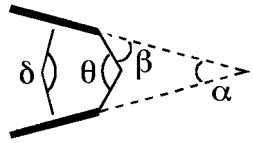

Figure 1. Common set of angles used to describe [1]metallocenophanes.

The identity of the bridging atom E in metallocenophanes and related species is one of the most important factors contributing to the degree of ring tilt (α), and consequently, the strain present. Thus, alteration of the covalent radius of the bridging element would be expected to allow the tilt angle and associated strain of [1]ferrocenophanes to be modulated. Indeed, since the report of the first sila[1]ferrocenophane (**1**, ER_x = $SiPh_2$) in 1975,[12] related species containing non-metallic main group elements (e.g., **1**, E = B, Ge, P, As, S, Se) and also main group metals (**1**, E = Al, Ga, Sn) in the bridge have been described.[1,2] This has allowed studies of highly strained metallorings with tilt angles of over 30° (**1**, E = B or S) through to analogs with much lower degrees of strain (e.g., **1**, E = Sn, α = 14°−15°).[1,2] A diverse range of reactivity has been identified for these species, including ring opening via cleavage of either the E−Cp or M−Cp bonds.[1,2,13]

Although a wide variety of metallocenophanes with main group elements in the bridge has now been studied in detail, analogous species with transition metals in the bridge are rare. Until recently, examples were limited to [1]ferrocenophanes **1** (ER_x = MCp_2, Cp = η^5-C_5H_5) containing the early d-block metals (M = Ti, Zr, Hf).[14] The trinuclear ferrocenophanes prepared by the alkali-metal-mediated manganation of ferrocene, however, also contain components where a single Mn(II) ion bridges a 1,1′-ferrocenediyl fragment.[15] In a recent preliminary communication[16] we reported the synthesis and characterization of a nickela[1]ferrocenophane (**4a**) and a platina[1]ferrocenophane (**4c**), the first examples of strained metallocenophanes with late transition metals in the bridge. In this paper, we describe the full details of our work on the synthesis, structures, and electronic properties of the three group 10 bridged [1]ferrocenophanes (Ni, **4a**; Pd, **4b**; Pt, **4c**). In addition, we describe the unprecedented reactivity of these interesting strained molecules.

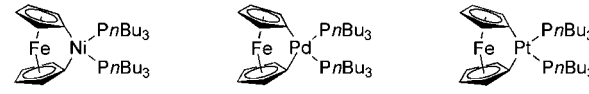

4a **4b** **4c**

2. Results and Discussion

2.1. Synthesis and Characterization of the Group 10 Bridged [1]Ferrocenophanes 4a, 4b, and 4c. The availability of dihalide complexes containing the elements of group 10 suggested that compounds **4a**, **4b**, and **4c** may be prepared by simple extension of the main synthetic route to mononuclear [1]ferrocenophanes.[1] Thus, the reaction of $Li_2[Fe(\eta^5$-$C_5H_4)_2]$·tmeda (**5**, tmeda = *N*,*N*,*N*′,*N*′-tetramethylethylenediamine) with *trans*-$[NiCl_2(P$*n*-$Bu_3)_2]$ (*trans*-**6a**) was attempted and this resulted in a cloudy, dark red mixture in hexanes at −20 °C. Analysis by $^{31}P\{^1H\}$ NMR spectroscopy immediately after the mixture had warmed to ambient temperature revealed *ca.* 20% conversion to a single new phosphorus-containing product (δ = 13.5 ppm). Prolonged stirring at room temperature did not result in further consumption of **6a**. Changing the reaction solvent to Et_2O, however, had a profound effect with $^{31}P\{^1H\}$ NMR spectroscopy indicating complete consumption of **6a** after warming to room temperature. In this instance, removal of solvent and recrystallization from hexanes afforded **4a** as dark orange crystals and in much improved isolated yield (40% compared to 11% in hexanes). Analysis of the mother liquors by $^{31}P\{^1H\}$ NMR spectroscopy indicated the presence of a new phosphorus-containing compound, the chemical shift (δ = −2 ppm) of which suggesting an acyclic formulation (*vide infra*).

In order to investigate the generality of the chloride metathesis reaction, *trans*-$[PdCl_2(P$*n*-$Bu_3)_2]$ (*trans*-**6b**) and *cis*-$[PtCl_2(P$*n*-

(6) Green, J. C. *Chem. Soc. Rev.* **1998**, *27*, 263.
(7) Barlow, S.; Drewitt, M. J.; Dijkstra, T.; Green, J. C.; O'Hare, D.; Whittingham, C.; Wynn, H. H.; Gates, D. P.; Manners, I.; Nelson, J. M.; Pudelski, J. K. *Organometallics* **1998**, *17*, 2113.
(8) (a) Fischer, A. B.; Kinney, J. B.; Staley, R. H.; Wrighton, M. S. *J. Am. Chem. Soc.* **1979**, *101*, 6501. (b) Bourke, S. C.; MacLachlan, M. J.; Lough, A. J.; Manners, I. *Chem.—Eur. J.* **2005**, *11*, 1989.
(9) (a) Foucher, D. A.; Tang, B. Z.; Manners, I. *J. Am. Chem. Soc.* **1992**, *114*, 6246. (b) Gómez-Elipe, P.; Macdonald, P. M.; Manners, I. *Angew. Chem., Int. Ed. Engl.* **1997**, *36*, 762. (c) Temple, K.; Jakle, F; Sheridan, J. B.; Manners, I. *J. Am. Chem. Soc.* **2001**, *123*, 1355. (d) Reddy, N. P.; Yamashita, H.; Tanaka, M. *Chem. Commun.* **1995**, *22*, 2263.
(10) (a) Rider, D. A.; Cavicchi, K. A.; Power-Billard, K. N.; Russell, T. P.; Manners, I. *Macromolecules* **2005**, *38*, 6931. (b) Tanabe, M.; Vandermeulen, G. W. M.; Chan, W. Y.; Cyr, P. W.; Vanderark, L.; Rider, D. A.; Manners, I. *Nat. Mater.* **2006**, *5*, 467.
(11) Polymetallocenes and related materials are also available through polycondensation approaches. For some recent examples, see: (a) Miles, D.; Ward, J.; Foucher, D. A. *Macromolecules* **2009**, *42*, 9199. (b) Scheibitz, M.; Li, H.; Schnorr, J.; Perucha, A. S.; Bolte, M.; Lerner, H.-W.; Jäkle, F.; Wagner, M. *J. Am. Chem. Soc.* **2009**, *131*, 16319.
(12) Osborne, A. G.; Whiteley, R. H. *J. Organomet. Chem.* **1975**, *101*, C27.
(13) (a) Mizuta, T.; Imamura, Y.; Miyoshi, K. *J. Am. Chem. Soc.* **2003**, *125*, 2068. (b) Herbert, D. H.; Tanabe, M.; Bourke, S. C.; Lough, A. J.; Manners, I. *J. Am. Chem. Soc.* **2008**, *130*, 4166.
(14) Broussier, R.; Da Rold, A.; Gautheron, B.; Dromzee, Y.; Jeannin, Y. *Inorg. Chem.* **1990**, *29*, 1817.
(15) (a) García-Álvarez, J.; Kennedy, A. R.; Klett, J.; Mulvey, R. E. *Angew. Chem., Int. Ed.* **2007**, *46*, 1105. (b) Blair, V. L.; Carrella, L. M.; Clegg, W.; Klett, J.; Mulvey, R. E.; Rentschler, E.; Russo, L. *Chem.—Eur. J.* **2009**, *15*, 856.
(16) Whittell, G. R.; Partridge, B. M.; Presly, O. C.; Adams, C. J.; Manners, I. *Angew. Chem., Int. Ed.* **2008**, *47*, 4354.

Scheme 1. Preparation of Group 10 Metal-Bridged [1]Ferrocenophanes

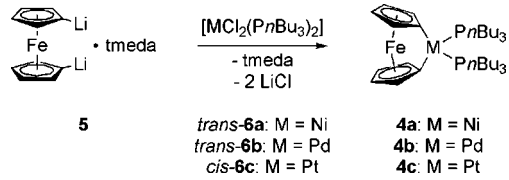

5 | *trans*-**6a**: M = Ni; *trans*-**6b**: M = Pd; *cis*-**6c**: M = Pt | **4a**: M = Ni; **4b**: M = Pd; **4c**: M = Pt

$Bu_3)_2$] (*cis*-**6c**) were treated with compound **5** (Scheme 1). In hexanes at −20 °C, both reactions afforded the respective dark red, crystalline metalla[1]ferrocenophanes, [{Fe(η^5-$C_5H_4)_2$}Pd(P*n*-$Bu_3)_2$] (**4b**) and [{Fe(η^5-$C_5H_4)_2$}Pt(P*n*-$Bu_3)_2$] (**4c**), albeit in modest to low yields (**4b**: 34% and **4c**: 13%). Unlike the nickel case however, exchanging the solvent for Et_2O had a negative effect on the reaction yields and even prevented the isolation of the pallada[1]ferrocenophane, **4b**. When **4a**, **4b**, and **4c** were recrystallized from hexanes, analysis of the mother liquors by $^{31}P\{^1H\}$ NMR spectroscopy revealed detectable quantities of these species, suggesting that their high solubilities in hexanes at low temperature also contributed to the observed low isolated yields. Interestingly, the treatment of *trans*-[$PtCl_2$(P*n*-$Bu_3)_2$] (*trans*-**6c**) with **5** afforded no reaction under the same conditions that proved successful for the conversion of *cis*-**6c**, as evidenced by $^{31}P\{^1H\}$ NMR spectroscopy. The *trans*- to *cis*-isomerization of **6a** and **6b** upon formation of the metalla[1]ferrocenophanes presumably reflects the increased stability of the *cis*-isomer on exchange of the chloride for a stronger *trans* influence ligand.[17] Although the electrostatic interactions between the ligands are calculated to be smaller in **6c**, thus reducing the energetic preference for the *trans*-isomer, it would appear that the activation barrier to isomerization is sufficiently high to prevent formation of **4c** from *trans*-**6c**.

Surprisingly, the relatively bulky P*n*-Bu_3 ligand proved to be important for the stabilization and isolation of these complexes. Attempts to synthesize nickel-, palladium- and platinum-bridged [1]ferrocenophanes bearing trimethylphosphine or chelating diphosphines as the ligand or ligands failed, and no isolable products were obtained.

2.1.1. Characterization of 4a, 4b, and 4c. ^1H, $^{13}C\{^1H\}$, and $^{31}P\{^1H\}$ NMR spectra recorded for the new [1]ferrocenophanes were in accord with the proposed structures. All spectra displayed resonances at predictable chemical shifts and as such were consistent with the incorporation of a diamagnetic square-planar group 10 metal center. In the ^1H NMR spectra of compounds **4a**, **4b**, and **4c**, the two sets of chemically inequivalent cyclopentadienyl protons give rise to different resonances. It should be noted, however, that the difference in the chemical shifts of the two sets of Cp protons for the three complexes ($\Delta\delta$ = 0.27, <0.01, and 0.05 ppm for **4a**, **4b**, and **4c**, respectively) is appreciably smaller than that for other [1]ferrocenophanes, especially for complexes **4b** and **4c** (*cf.* $\Delta\delta$ = 0.32 ppm for [Fe(η^5-$C_5H_4)_2SiMe_2$]).[18] The $^{13}C\{^1H\}$ NMR spectra of the three complexes provided the first indication of their strained nature. The *ipso*-carbon resonances of the cyclopentadienyl rings (δ = 54.1 for **4a**, 58.2 for **4b**, and 51.8 ppm for **4c**) appeared high-field shifted relative to the ^{13}C resonance of ferrocene (δ = 69 ppm).[19] This change is normally attributed to an increase in sp^3 character of these carbon atoms, as a result of a distortion away from the unstrained trigonal-planar geometry. The reverse effect was reported in the cases of [{Fe(η^5-$C_5H_4)_2$}M(η^5-C_5H_4tBu)$_2$] (M = Ti, Zr, and Hf), which display corresponding $^{13}C\{^1H\}$ resonances at δ = 179.8, 159.0, and 153.3 ppm, respectively. These complexes, however, were essentially unstrained, as suggested by the solid-state structure of the zirconium derivative (α = 6°),[14] The chemical shifts of the *ipso*-carbons, therefore, more closely resemble those of the α-carbons of σ-aryl complexes.

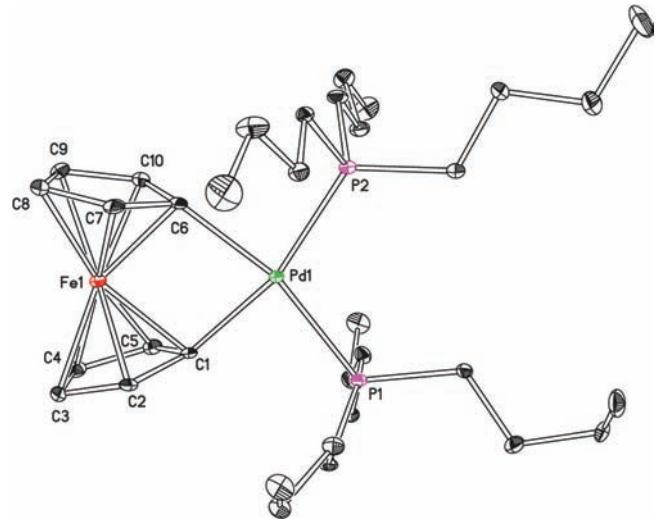

Figure 2. Molecular structure of **4b** with thermal ellipsoids at the 30% probability level. Selected bond lengths (Å) and angles (deg): Pd(1)−C(1), 2.086(4); Pd(1)−C(6), 2.094(5); Pd(1)−P(2), 2.2867(13); Pd(1)−P(1), 2.2906(13); Fe(1)−C(6), 2.004(4); Fe(1)−C(1), 2.009(4); Fe(1)−C(5), 2.014(5); Fe(1)−C(2), 2.016(4); Fe(1)−C(7), 2.020(5); Fe(1)−C(10), 2.018(5); Fe(1)−C(4), 2.056(5); Fe(1)−C(3), 2.061(4); Fe(1)−C(8), 2.058(5); Fe(1)−C(9), 2.070(5); C(1)−Pd(1)−C(6), 79.15(17); P(1)−Pd(1)−P(2), 109.21(5).

Table 1. Selected Structural Data for the Metalla[1]ferrocenophanes, [{(η-$C_5H_4)_2$Fe}M(P*n*-$Bu_3)_2$] (**4a**: M = Ni, **4b**: M = Pd, and **4c**: M = Pt)

	α [deg]	β [deg]	δ [deg]	θ [deg]	Fe−Cp centroid [Å]	Fe...M [Å]
M = Ni (**4a**)	28.4	25.5, 25.9	157.3	80.7(2)	1.62, 1.62	3.03
M = Pd (**4b**)	24.5	26.9, 27.1	160.3	79.15(17)	1.63, 1.63	3.11
M = Pt (**4c**)	25.2	26.4, 26.2	159.4	78.36(16)	1.64, 1.63	3.14

Unequivocal evidence for the solid-state structure of the metalla[1]ferrocenophanes **4a**, **4b**, and **4c** was provided by single crystal X-ray diffraction analysis. Figure 2 shows a thermal ellipsoid plot of **4b**, together with selected bond distances and angles (for representations of the optimized geometries of all three species, see Figures S4.1−S4.3). These compounds crystallized as red blocks in the monoclinic space group $P2_1/c$ upon cooling concentrated hexane solutions to −40 °C. All three crystals were isomorphous and contained one molecule per asymmetric unit with no short intermolecular interactions. The most relevant structural features pertaining to the strain induced by the *ansa*-bridge are the tilt angle α (**4a**: 28.4°; **4b**: 24.5°; **4c**: 25.2°) and the angle β (**4a**: 25.5°, 25.9°; **4b**: 26.9°, 27.1°; **4c**: 26.4°, 26.2°) (Table 1). As would be expected given the smaller covalent radius of nickel compared to that of palladium and platinum, complex **4a** exhibits the highest α angle in the solid state. The Fe−Cp(centroid) distances (1.62−1.65 Å) are similar to those found in the sila[1]ferrocenophane, [Fe(η^5-

(17) Harvey, J. N.; Heslop, K. M.; Orpen, A. G.; Pringle, P. G. *Chem. Commun.* **2003**, 278.
(18) Fischer, A. B.; Kinney, J. B.; Staley, R. H.; Wrighton, M. S. *J. Am. Chem. Soc.* **1979**, *101*, 6501.
(19) Lauterbur, P. C. *J. Am. Chem. Soc.* **1961**, *83*, 1838.

Table 2. Selected Angles and Distances for the Model Compounds [{(η-C_5H_4)$_2$Fe}M(PH_3)$_2$] (**7a**: M = Ni, **7b**: M = Pd, and **7c**: M = Pt)

	α [deg]	β [deg]	δ [deg]	θ [deg]	Fe−Cp [Å]	Fe−M [Å]
M = Ni (**7a**)	30.7	24.2	156.4	79.4	1.63	3.05
[M = Ni]$^+$ (**7a**$^+$)	39.8	17.4	145.2	74.9	1.68	3.21
M = Pd (**7b**)	27.0	25.1	159.5	77.3	1.65	3.17
[M = Pd]$^+$ (**7b**$^+$)	31.0	21.6	152.1	78.2	1.69	3.21
M = Pt (**7c**)	25.4	25.5	160.8	76.4	1.64	3.20
[M = Pt]$^+$ (**7c**$^+$)	31.0	21.7	152.1	74.6	1.70	3.32

$C_5H_4)_2SiMe_2$] (both 1.63 Å),[20] although this parameter varies little with the strength of the Fe−Cp bonds.[21] It has been shown, however, that an increase in the strength of the Fe−Cp bonds is manifested in less ring tilt and greater distortion of the *ipso*-carbon atoms (lower α and higher β angles), since deviation of the Cp rings from planarity leads to greater bond energy losses.[21] In the case of complexes **4a**, **4b**, and **4c**, the converse was true (lower β and higher α angles with respect to dimethylsila[1]ferrocenophane), suggesting that the Fe−Cp bonding is weaker in the former compounds than in **1** (ER_x = $SiMe_2$). The nickel, palladium, and platinum centers display a distorted square-planar geometry, with smaller C(*ipso*)−M−C(*ipso*) angles (θ) (80.7(2)°, 79.15(17)°, and 78.36(16)°, respectively) and larger P−M−P angles [109.56(6)°, 109.21(5)°, 108.75(4)°] than would be found in the ideal geometry (90°). It is noteworthy that these represent the first [1]ferrocenophanes to contain an element with a square-planar geometry in the *ansa*-bridge, as would be expected for d^8 metal complexes containing strong field ligands.

The geometries of **4a**−**c** and their respective cations were modeled with C_{2v} symmetry substituting PH_3 for P*n*-Bu_3 (**7a**−**c** and **7a**$^+$−**7c**$^+$). The resultant optimized geometries are given in Table 2. The good agreement of the calculated and crystallographic structural data establishes that the simplified compounds provide an accurate model for these complexes in spite of the substitution of PH_3 for P*n*-Bu_3.

2.2. Electronic Structures of Metalla[1]ferrocenophanes 4a, 4b, and 4c. The electronic properties of ferrocene and its derivatives have been studied extensively by UV/vis spectroscopy. These compounds give rise to six bands,[22] with those that appear at *ca.* 325 (band III) and 440 nm (band II) having attracted the most attention. The highest energy UV/vis absorption in ferrocene (band IV) at 270 nm has been assigned to a ligand-to-metal charge transfer transition, whereas the weaker absorptions at 325 and 440 nm (bands III and II) have been attributed to transitions between the filled HOMOs and the LUMO, which are predominantly d−d in nature and therefore Laporte forbidden. The absorption at 440 nm has been assigned to two closely spaced transitions (bands IIa and IIb) of which the lowest energy component (IIa) has been shown to undergo a dramatic red shift in [1]ferrocenophanes,[1] since the HOMO−LUMO gap decreases significantly as ring tilt increases. In addition, the greater intensity of bands III and II for ferrocenophanes, relative to ferrocene, can be explained by the relaxation of the Laporte selection rule on reduction of the molecular symmetry.[23] To obtain information on the electronic structure of the group 10 bridged [1]ferrocenophanes, solution-phase UV/vis spectra in the 200−800 nm range were collected for species **4a**−**c** (Figure 3). The UV/vis spectra of the nickela- and platina[1]ferrocenophanes **4a** and **4c**, which exhibit a red-shifted transition (band II, in comparison to the spectrum of ferrocene) at 478 (ϵ = 873 M^{-1} cm^{-1}) and 493 nm (ϵ = 264 M^{-1} cm^{-1}), respectively, are consistent with ring-tilted structures. In the UV/vis spectrum of the palladium derivative **4b**, however, band II appears as a poorly resolved shoulder on a more intense, higher energy band at 406 nm (ϵ = 537 M^{-1} cm^{-1}) and, as such, could not be precisely located (*ca.* 500 nm). Nonetheless, the HOMO−LUMO gap of **4b** would appear to have decreased relative to that in ferrocene, as expected for a ring-tilted structure.

Orbital energies for the neutral compounds, **7a**−**c**, are listed in Table 3 together with those for [Fe(η^5-C_5H_4)$_2$$SiMe_2$] (**1**, ER_x = $SiMe_2$) for comparison. The top three occupied orbitals are all Fe localized (Figure 4) and closely resemble those found for other ferrocenophanes.[7] The HOMO−LUMO energy gap is significantly larger for the $SiMe_2$ bridged compound than for the group 10 metal-bridged ferrocenophanes, consistent with the lower energy found for the absorption bands of the latter species. The decrease in the gap is in part due to the higher energy of the Fe d orbitals, which can be attributed to the inductive effect of the bridging group. The nature of the LUMO in **7a**−**c** is also different. Whereas **7a**−**c** have a LUMO with MC_2P_2 antibonding characteristics, the $SiMe_2$ bridged compound has an Fe−Cp antibonding orbital descended from the e_{1g}* orbitals of ferrocene.

The ferrocenophanes **4a**, **4b**, and **4c** were analyzed by cyclic voltammetry in order to study any electronic effects on the ferrocene/ferrocenium redox couple associated with the *bis*-(phosphine)metal(II) bridging unit. Figure 5 shows the cyclic voltammograms obtained from analyses of 1.0×10^{-3} mol dm^{-3} dichloromethane solutions of **4a**, **4b**, and **4c** which were in 0.1 mol dm^{-3} [Bu_4N][PF_6]. The voltammograms were obtained at a scan rate of 250 mV s^{-1}, and potentials are referenced to that of the ferrocene/ferrocenium redox couple. As can be seen in Figure 5, the platinum-containing compound **4c** undergoes a chemically reversible (i_{pa}/i_{pc} = 1) one-electron oxidation, as previously found for sila[1]-,[21] germa[1]-,[24] and stanna[1]ferrocenophanes.[2e] This is in contrast with the result obtained for complexes **4a** and **4b**, which exhibited chemically irreversible redox behavior. A notable feature of each voltammogram was the shift to negative oxidation potentials [E_p = −0.821, −0.658, and −0.628 V ($E_{1/2}$ = −0.682 V) for compounds **4a**, **4b**, and **4c**, respectively]. Unlike the latter compounds, **1** (ER_x = $SiMe_2$) exhibits a half-wave oxidation potential almost identical to that of ferrocene despite displaying an appreciable degree of ring tilt [α = 20.8(5)°]. Thus, it seems unlikely that the observed cathodic shifts can be connected with distortion of the ferrocenediyl group. Cathodic shifts have previously been observed upon increased methylation of the Cp rings and attributed to transmission of the electron-donating properties of the methyl groups to the iron center.[21] Moreover, such changes have been correlated with decreasing ring tilt, but analysis of the solid-state structures of **4a**, **4b**, and **4c** shows the converse to be true. A dative interaction from the *bis*(pho-

(20) Finckh, W.; Tang, B. Z.; Foucher, D. A.; Zamble, D. B.; Ziembinski, R.; Lough, A.; Manners, I. *Organometallics* **1993**, *12*, 823.
(21) Pudelski, J. K.; Foucher, D. A.; Honeyman, C. H.; Lough, A. J.; Manners, I.; Barlow, S.; O'Hare, D. *Organometallics* **1995**, *14*, 2470.
(22) Sohn, Y. S.; Hendrickson, D. N.; Gray, H. B. *J. Am. Chem. Soc.* **1971**, *93*, 3603.
(23) Rulkens, R.; Gates, D. P.; Balaishis, D.; Pudelski, J. K.; McIntosh, D. F.; Lough, A. J.; Manners, I. *J. Am. Chem. Soc.* **1997**, *119*, 10976.
(24) Castruita, M.; Cervantes-Lee, F.; Mahmoud, J. S.; Zhang, Y.; Pannell, K. H. *J. Organomet. Chem.* **2001**, *637*−*639*, 664.

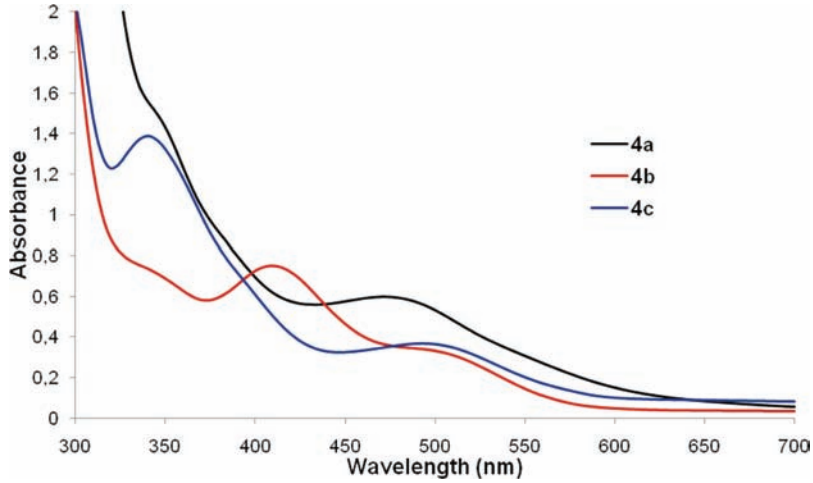

Figure 3. UV/vis spectra of metalla[1]ferrocenophanes in *n*-hexanes (**4a**, 0.5 mM; **4b**, 1.3 mM; **4c**, 1.0 mM).

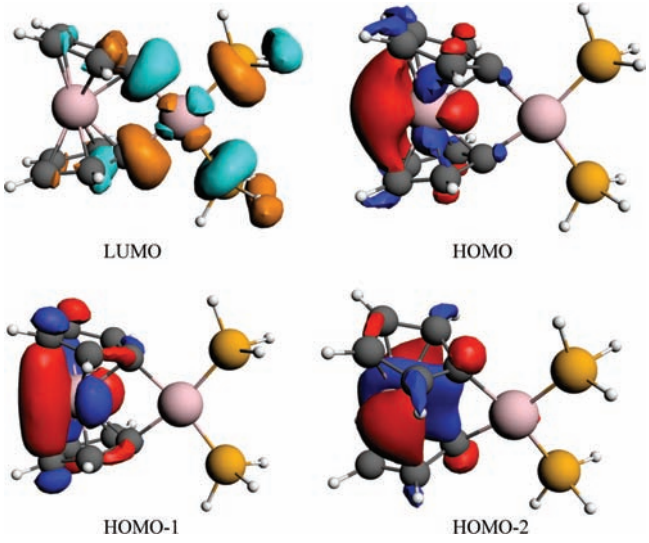

Figure 4. Isosurfaces for selected orbitals of **7a**. Those for **7b** and **7c** are similar.

Table 3. Orbital Energies (eV) and Calculated Ionization Energies (eV) for (**7a**−**c** and **1**, $ER_x = SiMe_2$)

	Ni (**7a**)	Pd (**7b**)	Pt (**7c**)	**1**, ($ER_x = SiMe_2$)
LUMO	−2.01	−2.02	−1.75	−1.44
HOMO	−3.39	−3.38	−3.32	−4.19
HOMO−1	−3.45	−3.42	−3.33	−4.22
HOMO−2	−3.83	−3.75	−3.67	−4.67
IE	5.67	5.74	5.73	6.85

sphine)metal fragment to the iron center could stabilize the iron(III) complex and consequently lead to the observed cathodic shift of the oxidation potential. The spatial separation between the two metal centers in each compound, however, is at least 27% longer than the sum of the covalent radii.[25] It is noteworthy that while the Fe···Si interaction is also larger than the sum of the covalent radii (by 18%) in [Fe(η^5-C_5H_4)$_2$$SiMe_2$], the ^{57}Fe Mossbauer spectrum suggested the possibility of a dative interaction between silicon and iron.[21] Nevertheless, this feature did not result in the expected shift of the oxidation potential, making it difficult to invoke such an argument for the marked

(25) Cordero, B.; Gómez, V.; Platero-Prats, A. E.; Revés, M.; Echeverría, J.; Cremades, E.; Barragán, F.; Alvarez, S. *Dalton Trans.* **2008**, 2832.

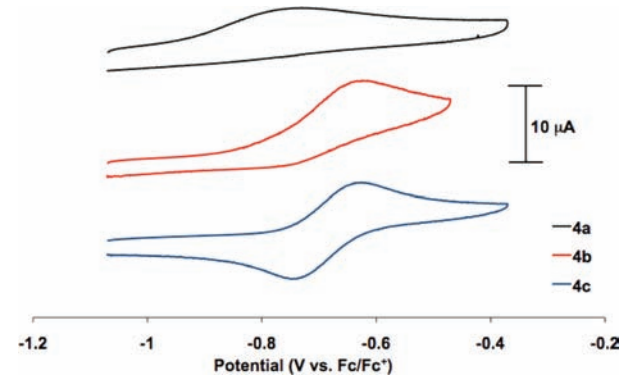

Figure 5. Cyclic voltammograms of **4a**, **4b**, and **4c** as 1×10^{-3} mol dm^{-3} solutions in CH_2Cl_2 which were 0.1 mol dm^{-3} in [N*n*Bu$_4$][PF$_6$] (scan rate = 250 mV s^{-1}).

Table 4. Calculated Fe−M Bond Orders

	Wiberg	NAO[a]	MO[b]
Ni	0.0165	0.0012	−0.0315
Pd	0.0158	−0.0009	−0.0503
Pt	0.0148	0.001	−0.0608
$SiMe_2$	0.0353	0.0975	0.2463

[a] Atom−atom overlap-weighted Natural Atomic Orbital (NAO) bond order. [b] NBO calculated MO bond order.

changes in the oxidation potentials for complexes **4a**−**c** given the larger effective interatomic separation. In order to probe the existence of a direct interaction between the Fe and the group 10 metal further, an AIM (atoms in molecules) analysis was performed. In each of the three neutral molecules, **7a**−**c**, a (3,1) critical point was identified between the Fe and the group 10 metal indicating the center of a ring rather than the existence of a direct interaction. NBO (natural bond order) analysis also failed to find any significant direct bonding interaction between Fe and the group 10 metal (Table 4).

The gas phase vertical ionization energies (IEs) were calculated as 5.67, (**7a**) 5.74 (**7b**), and 5.73 eV (**7c**) (Table 3). These values are significantly lower than the $SiMe_2$ bridged compound, which has calculated and experimental first IEs of 6.85 and 6.84 eV, respectively.[7] This is in good agreement with the striking reduction in oxidation potential found for **4a**−**c**. On ionization (**7a**$^+$−**7c**$^+$) the spin density was located on the Fe atom with a hole in the neutral molecules' HOMO. The orbital energies (Table 3) suggest that the principal origin of the lowering of

the oxidation potential is the greater electron-donating effect of the M(P*n*-Bu$_3$)$_2$ groups compared with SiMe$_2$. In addition the greater polarizability of the former group will also stabilize preferentially the positive charge in the metal-bridged ferrocenophane cations.[26]

2.3. Ring-Opening Reactions of Metalla[1]ferrocenophanes 4a, 4b, and 4c. The highly strained nature of compounds **4a**, **4b**, and **4c**, as revealed by the X-ray analyses and suggested by UV/vis spectroscopy, prompted us to explore their ring-opening behavior. Primarily, we were interested in establishing whether the new metalla[1]ferrocenophanes may lead to the formation of polymers by ROP, as has been observed for other [1]ferrocenophanes **1** (E = Si, Ge, P, S, B), or if other unusual reactivity would ensue.

2.3.1. Attempted Thermal ROP of 4a, 4b, and 4c. The thermal behavior of all three complexes was studied by differential scanning calorimetry (DSC). A first-order endothermic transition, presumably corresponding to the melting process, was observed at 137, 140, and 146 °C for **4a**, **4b**, and **4c**, respectively. For complexes **4a** and **4c**, the thermograms did not exhibit any further feature that would be consistent with an exothermic ring-opening process. Instead, another first-order endothermic transition was detected slightly above 200 °C. To investigate whether our inability to detect ROP by DSC was due to the slow rate of such a reaction, samples of **4a** and **4c** were heated in evacuated sealed tubes and the resulting materials were analyzed by $^{31}P\{^1H\}$ NMR spectroscopy. In both cases, the starting material remained unchanged after heating in the melt at 150 °C for 18 h. Further heating above 200 °C, however, resulted in a brown solid forming from the melt. $^{31}P\{^1H\}$ NMR spectroscopy revealed P*n*-Bu$_3$ to be the only phosphorus-containing component of this mixture, which suggests that the endothermic process observed above 200 °C by DSC can be assigned to phosphine dissociation. In contrast, the DSC thermogram of the palladium derivative **4b** (see Figure S1.1) exhibited a first-order exothermic transition at 145 °C subsequent to the melt endotherm at 140 °C, which was suggestive of a ROP process. When **4b** was heated in an evacuated, sealed tube at 150 °C, a new product was obtained, which was found to be highly air-sensitive. Analysis by $^{31}P\{^1H\}$ NMR spectroscopy showed a new, broad signal at δ 0.9 ppm, and the ^1H NMR spectrum displayed a very broad resonance in the Cp region, as well as signals corresponding to the *n*-Bu groups of the phosphine ligands. In accord with these data, it seemed reasonable to assume that a ring-opening process had taken place upon heating **4b**. Unfortunately, further analysis of this product was frustrated by the instability of the material and decomposition occurred on attempted isolation.

2.3.2. Anionic Ring-Opening Reactions. Synthesis of Complexes 8a and 8b. In view of the large α angle present in the three structures, which suggested a weakening of the Fe−Cp bonds, our initial attempts focused on the use of NaCp-initiated photolytic ROP.[10b,27] In this living polymerization, a moderately basic initiator cleaves the iron−cyclopentadienyl bond in a photoexcited monomer, thus differing from the alkyl or aryl lithium-initiated process, where the bridging atom−Cp bond is broken.[28] Rather surprisingly, none of the three complexes **4a**−**c** reacted with NaCp under the same conditions that successfully

Scheme 2. Syntheses and Decomposition Pathway of Complexes **8a** and **8b**

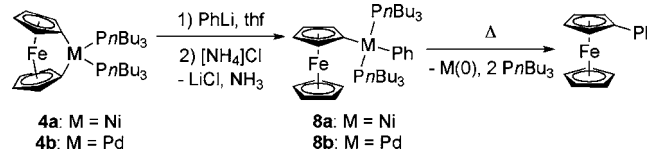

4a: M = Ni
4b: M = Pd
8a: M = Ni
8b: M = Pd

afford ring-opened products with sila- and phospha[1]ferrocenophanes and dicarba[2]ferrocenophanes.[29] Further attempts to ring open **4a**, **4b**, and **4c** involved the use of organolithium compounds, which have successfully been employed as initiators for the ROP of other ferrocenophanes.[30] However, the platinum derivative **4c** exhibited no reaction with PhLi and *n*-BuLi, even when stirred with 10 equiv of the latter for 18 h.

As would be expected on the grounds of metal−carbon bond strength, the nickela- and pallada[1]ferrocenophanes **4a** and **4b** proved more reactive than their platinum counterpart **4c**. Addition of 1 equiv of PhLi to a thf solution of **4a** or **4b** afforded a new product, characterized by a single resonance in the $^{31}P\{^1H\}$ NMR spectrum (δ −2 ppm for **4a** and 1 ppm for **4b**). After stirring for 7 days at room temperature, however, 50% of **4a** remained unreacted. In each case, the addition of a second equivalent of PhLi resulted in complete conversion to the new product after stirring for a further *ca.* 4 h. Quenching the reaction with ammonium chloride, filtration and evaporation of the solvent *in vacuo* yielded a black residue. Unfortunately, the high solubility of these materials in common organic solvents prevented successful purification by recrystallization. ^1H NMR spectra recorded of the black crudes, however, were in accord with acyclic, phenylated formulations for compounds **8a** and **8b**. For both complexes, these spectra showed two sets of signals corresponding to the two chemically inequivalent Cp rings, at δ 4.5 and 4.1 ppm integrating for 2 H each and δ 3.9 ppm for 5 H, together with the characteristic resonances for the phenyl and *n*-butyl groups. The proposed structures for these products are shown in Scheme 2. In view of the $^{31}P\{^1H\}$ NMR spectra, which exhibit one singlet in each case, the two phosphines must adopt a mutually *trans* arrangement and this requires ring-opening to be succeeded by isomerization at the group 10 metal.

Attempts to purify complexes **8a** and **8b** by sublimation from the black residues failed. For example, complex **8a** decomposed by reductive elimination of phenylferrocene from the metal center with concomitant release of phosphine (Scheme 2). This is not surprising, since diarylnickel(II) complexes of the type [NiPh$_2$(PR$_3$)$_2$] have been found to be thermally unstable, decomposing in solution and in air.[31] In accordance with these observations, attempts to prepare complex **8a** by reacting *trans*-[Ni(Ph)(Cl)(P*n*-Bu$_3$)$_2$][32] with Li[Fe(η^5-C$_5$H$_4$)(η^5-C$_5$H$_5$)]·tmeda (**9**) did not allow for isolation of the desired product. Instead, decomposition to free phosphine and phenylferrocene took place, thereby indicating the inherent instability of complex **8a**.

(26) Zachmanoglou, C. E.; Docrat, A.; Bridgewater, B. M.; Parkin, G.; Brandow, G.; Bercaw, J. E.; Jardine, C. N.; Lyall, M.; Green, J. C.; Keister, J. B. *J. Am. Chem. Soc.* **2002**, *124*, 9525.
(27) Tanabe, M.; Manners, I. *J. Am. Chem. Soc.* **2004**, *126*, 11434.
(28) Ni, Y.; Rulkens, R.; Manners, I. *J. Am. Chem. Soc.* **1996**, *118*, 4102.
(29) (a) Herbert, D. E.; Mayer, U. F. J.; Gilroy, J. B.; López-Gómez, M. J.; Lough, A. J.; Charmant, J. P, H.; Manners, I. *Chem.—Eur. J.* **2009**, *15*, 12234. (b) Patra, S. K.; Whittell, G. R.; Nagiah, S.; Ho, C.-L.; Wong, W.-Y; Manners, I. *Chem.—Eur. J.* **2010**, *16*, 3240.
(30) (a) Peckham, T. J.; Massey, J. A.; Honeyman, C. H.; Manners, I. *Macromolecules* **1999**, *32*, 2830. (b) Ieong, N. S.; Manners, I. *Macromol. Chem. Phys.* **2009**, *210*, 1080.
(31) (a) Chatt, J.; Shaw, B. L. *J. Chem. Soc.* **1960**, 1718. (b) Heinicke, J.; Peuleckea, N.; Kindermanna, M. K.; Jones, P. G. *Z. Anorg. Allg. Chem.* **2005**, *631*, 67.
(32) Complex *trans*-[NiPh(Cl)(P*n*-Bu$_3$)$_2$] was prepared following a reported procedure for *trans*-[NiPh(Cl)(PMe$_3$)$_2$]: Carmona, E.; Paneque, M.; Poveda, M. L. *Polyhedron* **1989**, *8*, 285.

To investigate whether the anionic ring-opening reaction could be accelerated by using more basic initiators, alkyl lithium reagents were evaluated. Complex **4b** remained unchanged after addition of 1 equiv of *n*-BuLi in thf, diethyl ether, or dimethoxyethane as solvent, even when the reaction mixture was stirred for 2 days with a crown ether or tmeda. Nonetheless, addition of 2 equiv of *n*-BuLi and 2 equiv of tmeda afforded 66% conversion of **4b** after 7 days of stirring at room temperature. Addition of another equivalent of *n*-BuLi and tmeda and stirring for a further 2 days, however, caused decomposition, as free phosphine was also observed by $^{31}P\{^1H\}$ NMR spectroscopy. Since β-hydride elimination may be expected to provide a low energy pathway by which any palladium *n*-butyl complex so formed may decompose, the reaction was repeated with *sec*-BuLi.[33] Similar results to those with *n*-BuLi, however, were obtained. It is interesting to note the greater reactivity of PhLi toward **4b** compared to that of *n*-BuLi. Although the former lithiated compound exhibits a lower degree of aggregation in thf solutions than the latter,[34] the reactivity of *n*-BuLi toward **4b** does not increase upon addition of complexing ligands such as 12-crown-4 or tmeda. Other factors, such as the ease of approach to the metal center by the flat phenyl anion, cannot be ruled out at this stage.

Despite the strained nature of the metalla[1]ferrocenophanes **4a**−**c**, the reactions of these complexes with anionic initiators did not afford the expected polymers. With the exception of the platinum derivative **4c**, however, the other two compounds, **4a** and **4b,** did undergo ring-opening reactions but with no evidence for chain propagation.[35]

2.3.3. Protonolysis of the Group 10 Metal−Carbon Bonds in 4a−4c. In view of the limited reactivity exhibited by **4a**, **4b**, and **4c** toward nucleophiles, we chose to investigate their chemistry toward protons and other electrophiles. By way of comparison, the stoichometric reaction of sila[1]ferrocenophanes with protic reagents leads to ring-opened species through Si−Cp bond cleavage.[1,8] Moreover, the electrophilic cleavage of the metal−carbon bonds in late transition metal alkyls or aryls upon reaction with a proton source has been studied extensively[36] and constitutes a synthetic route to group 10 monoalkyl or aryl complexes by stoichiometric protonolysis of the corresponding bialkyls or biaryls.[37]

Addition of 1 equiv of an ethereal solution of HCl to **4b** caused partial conversion of the starting material to a new complex. The addition of a further equivalent of acid, however, resulted in complete conversion. Spectroscopic analysis of the product revealed that *trans*-[$PdCl_2$(P*n*-Bu_3)$_2$] (**6b**) was obtained, indicating that the reaction was not selective to one metal−carbon bond, even when it is carried out with a deficit of HCl and at low temperature.

Scheme 3. Insertion of CO into a Pd−C Bond of Complex **4b**

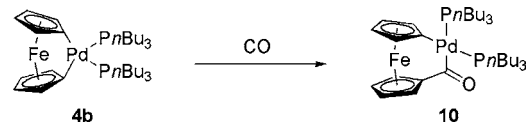

4b **10**

Similar results were obtained when reacting any of the metalla[1]ferrocenophanes with compounds containing heteroatom−hydrogen bonds such as thiophenol, phenol, methanol, and methylphenylamine. On the other hand, monitoring of the reaction of the group 10 metalla[1]ferrocenophanes with electrophiles, such as methyl iodide and trimethylsilyl triflate, by $^{31}P\{^1H\}$ NMR spectroscopy showed a complex mixture of unidentified products.

2.4. Insertion Reactions of Metalla[1]ferrocenophanes 4a, 4b, and 4c with CO. The reaction of group 10 alkyl or aryl complexes with small unsaturated molecules, such as carbon monoxide, alkynes, or alkenes, is of fundamental interest since it constitutes a key step in many industrial processes such as polyolefin and polyketone production, olefin oligomerization and co-oligomerization, and carbonylation/alkoxycarbonylation of alkenes and alkynes.[38] These reactions can be regarded as migratory insertions, which involve coordination of the small molecule to the metal center, followed by intramolecular insertion of the alkyl or aryl ligand into the multiple bonds. In the case of metallacycles, this sequence leads to ring expansion rather than the chain growth that results from acyclic complexes. In order to investigate the behavior of the metalla[1]ferrocenophanes under similar conditions, we attempted the reactions of **4a**−**c** with CO.

Carbon monoxide was bubbled through a toluene solution of **4b** at room temperature for 2−3 min, and the reaction mixture was analyzed by $^{31}P\{^1H\}$ NMR spectroscopy. The spectrum exhibited two doublets at δ 5.8 and −0.5 ppm ($^2J_{PP}$ = 32 Hz), as expected for a complex bearing two inequivalent phosphine ligands, while the ^1H NMR spectrum contained two sets of two signals each corresponding to the now chemically inequivalent cyclopentadienyl rings (see Supporting Information). Furthermore, the formation of an acyl ligand was evidenced by the appearance of a strong IR absorption at 1736 cm^{-1}. When taken collectively, the solution-phase spectroscopic data suggested insertion of CO into a single Pd−C bond (Scheme 3), the product of which could be isolated in good yield (71%). Crystals suitable for X-ray diffraction were obtained by slow evaporation of a hexane solution. The crystal structure of **10** confirmed the deductions made on the basis of solution-phase spectroscopy and is shown in Figure 6. In keeping with the expectations of ring expansion, the ferrocenyl moiety is much less strained than in the case of **4b**, with a ring tilt angle, α, of 13.7°. Other structural features, including the Fe−Cp (centroid) distances (1.63−1.64 Å), are very similar to those found in complex **4b**.

In the case of the nickel derivative **4a**, the reaction proceeded differently. After treatment with CO, in a similar manner to **4b**, the $^{31}P\{^1H\}$ NMR spectrum of the reaction mixture exhibited only one resonance (δ 13.3 ppm). The frequency of this signal

(33) Crabtree, R. H. *The Organometallic Chemistry of the Transition Metals*; John Wiley & Sons, Inc.: Hoboken, NJ, 2005.

(34) (a) Reich, H. J.; Green, D. P.; Medina, M. A.; Goldenberg, W. S.; Gudmundsson, B. Ö.; Dykstra, R. R.; Phillips, N. H. *J. Am. Chem. Soc.* **1998**, *120*, 7201. (b) Smith, M. B.; March, J. *March's Advanced Organic Chemistry*, 5th ed.; John Wiley & Sons, Inc.: New York, 2001.

(35) To gain further insight into this process, the reaction of the pallada[1]ferrocenophane **4b** with Li[Fe(η^5-C_5H_4)(η^5-C_5H_5)]·tmeda, which resembles the proposed propagating species of a living polymer chain, was carried out. After 6 days of stirring equimolar amounts of the two compounds in thf at room temperature, only partial conversion (30%) to a unidentified product was observed by $^{31}P\{^1H\}$ NMR spectroscopy. This result suggests that the low reactivity of the complexes **4a** and **4b** towards the lithiated ring-opened monomer hinders the formation of polymer.

(36) For example, see: (a) Romeo, R.; Plutino, M. R.; Elding, L. I. *Inorg. Chem.* **1997**, *36*, 5909. (b) Stahl, S. S.; Labinger, J. A.; Bercaw, J. E. *J. Am. Chem. Soc.* **1996**, *118*, 5961. (c) Romeo, R.; D'Amico, G. *Organometallics* **2006**, *25*, 3435.

(37) (a) Shekhar, S.; Hartwig, J. F. *J. Am. Chem. Soc.* **2004**, *126*, 13016. (b) Cámpora, J.; Matas, I.; Palma, P.; Graiff, C.; Tiripicchio, A. *Organometallics* **2005**, *24*, 2827.

(38) Cavell, K. J. *Coord. Chem. Rev.* **1996**, *155*, 209.

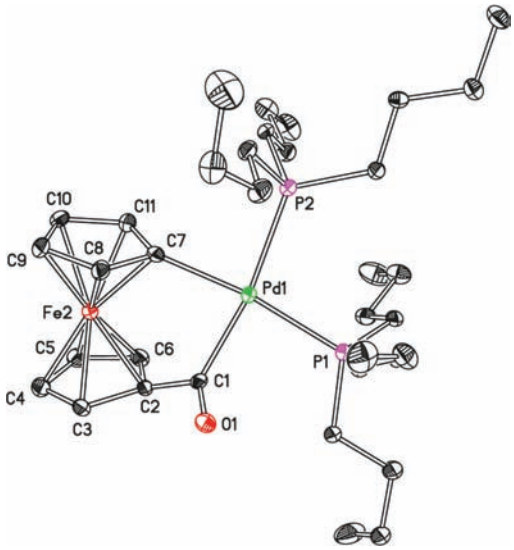

Figure 6. Molecular structure of complex **10** with thermal ellipsoids at the 30% probability level. Selected bond lengths (Å) and angles (deg): Pd(1)−C(1), 2.057(4); Pd(1)−C(7), 2.095(4); Pd(1)−P(1), 2.3162(10); Pd(1)−P(2), 2.3664(11); Fe(2)−C(2), 1.982(4); Fe(2)−C(6), 1.999(5); Fe(2)−C(11), 2.030(4); Fe(2)−C(3), 2.032(4); Fe(2)−C(8), 2.036(5); Fe(2)−C(9), 2.043(5); Fe(2)−C(10), 2.044(4); Fe(2)−C(7), 2.049(4); Fe(2)−C(4), 2.070(4); Fe(2)−C(5), 2.075(5); C(1)−Pd(1)−C(7), 83.38(15); P(1)−Pd(1)−P(2), 102.34(4).

is comparable to that reported for $[Ni(CO)_2(P\textit{n}\text{-}Bu_3)_2]$ (δ 12.1 ppm)[39] and suggested that reductive carbonylation occurred instead of migratory insertion. Furthermore, this result is consistent with the reactivity found in other metallacycles and acyclic complexes of nickel containing phosphine ligands.[40] In contrast, the platinum derivative **4c** proved unreactive toward CO under the same conditions that for **4b** afforded complex **10**.

2.5. Oxidatively-Induced Intramolecular Cyclopentadienyl Ligand Coupling Reactions of Metalla[1]ferrocenophanes 4a−c: Synthesis of [5,5′]Bicyclopentadienylidene (Pentafulvalene) π-Complexes of Nickel, Palladium, and Platinum(0). As mentioned above, the nickela- and pallada[1]ferrocenophane **4a** and **4b** exhibit electrochemically irreversible redox behavior, a feature normally attributed to the low stability of the cationic species stemming from the one-electron oxidation of the iron center. However, this result is in contrast to the reversible electrochemistry found in the case of the platinum derivative **4c**. Moreover, the oxidation potentials of all three complexes exhibit a cathodic shift with respect to that of ferrocene and dimethylsila[1]ferrocenophane (**1**, $ER_x = SiMe_2$).[21] In order to understand the differences in the redox behavior of these complexes, we sought to identify the products of chemical oxidation. Whereas the reaction of **4b** with 1 equiv of ferrocenium tetrafluoroborate afforded a complex mixture of unidentified products, the use of other oxidants, such as O_2 and S_8, had a different outcome. Thus, the $^{31}P\{^1H\}$ NMR spectrum of the reaction between **4b** and oxygen showed conversion of the starting material to a new product (δ 1.7 ppm), which was obtained together with tri-*n*-butylphosphine oxide (δ 49.0 ppm)[41]

Scheme 4. Reaction of Complexes **4b** and **4c** with Elemental Sulfur

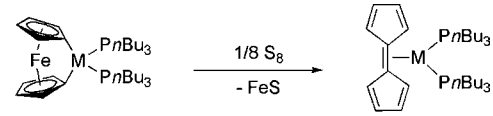

4b: M = Pd
4c: M = Pt

11b: M = Pd
11c: M = Pt

and a dark precipitate. The variable amounts of $OP\textit{n}\text{-}Bu_3$ formed, however, hindered the isolation of the new product. Assuming that the dark precipitate might be iron oxide, we attempted to control the reaction stoichiometry further by using pyridine-*N*-oxide instead of molecular oxygen. The former compound has commonly been used in the preparation of transition metal oxo complexes.[42] Moreover, it has been reported that the reaction of the complex $[(C_5Me_5)_2U(I)(thf)]$ with KC_8 and pyridine-*N*-oxide leads to the formation of the dimer, $(C_5Me_5)_2$, and uranium oxides, presumably through an unstable $[(C_5Me_5)_2U(=O)_2]$ complex that is reduced by the $[C_5Me_5]^-$ ligand.[43] In this case, however, the pyridine-*N*-oxide merely acts as an oxygen donor to the phosphorus ligands, and $OP\textit{n}\text{-}Bu_3$ was the only phosphorus-containing product obtained. In contrast, the reaction of **4b** with 1 equiv of sulfur atoms readily afforded the previously detected product [$\delta(^{31}P)$ 1.7 ppm] upon stirring at room temperature for 10 min. Again, a dark precipitate was also formed, most likely iron sulfide (see Supporting Information). In this case the formation of $SP\textit{n}\text{-}Bu_3$ was also observed,[41] which stems from the further reaction of the initial product with sulfur.[44] A slight excess of sulfur atoms (*ca.* 1.1 equiv) was therefore required to consume all the starting ferrocenophane, and conducting the reaction at low temperature (−78 °C) reduced the amount of $SPBu_3$ formed to less than 15% of the phosphorus-containing products. After separation from the precipitate and recrystallization from hexane, the product was obtained as a burgundy crystalline solid in 52% yield and ultimately identified as the η^2-[5,5′]bicyclopentadienylidene (pentafulvalene) complex **11b** (Scheme 4). The analogous platinum derivative can be readily prepared following a similar procedure from the platina[1]ferrocenophane **4c**. The amount of $SP\textit{n}\text{-}Bu_3$ obtained, however, was reduced to less than 10% of the phosphorus-containing products. Recrystallization from hexanes at −40 °C afforded the [5,5′]bicyclopentadienylidene complex **11c** as orange crystals in 73% yield.

Compound **11b** crystallized in the monoclinic space group $P2_1/n$ and pertinent geometrical parameters for this structure are included in Figure 7. The geometry about the palladium center is best described as trigonal planar with the C1−C6 bond vector lying in the PdP_2 plane. The bond lengths for C2−C3, C4−C5, C7−C8, and C9−C10 range from 1.359(3) to 1.366(3) Å and as such are consistent with double bonds.[45] These alternate with C−C distances around the rings of between 1.433(3) and 1.459(3) Å, which are lengths characteristic of $C(sp^2)-C(sp^2)$ single bonds. The C1−C6 bond distance [1.440(3)

(39) Meriwether, L. S.; Leto, J. R. *J. Am. Chem. Soc.* **1961**, *83*, 3192.
(40) (a) Cámpora, J.; Maya, C. M.; Palma, P.; Carmona, E.; Gutiérrez-Puebla, E.; Ruiz, C.; Graiff, C.; Tiripicchio, A. *Chem.—Eur. J.* **2005**, *11*, 6889. (b) Maya, C. M.; Cámpora, J.; Carmona, E.; Matas, I.; Palma, P.; Gutiérrez-Puebla, E.; Monge., A. *Chem.—Eur. J* **2007**, *13*, 3675. (c) Cámpora, J.; Matas, I.; Palma, P.; Álvarez, E.; Graiff, C.; Tiripicchio, A. *Organometallics* **2007**, *26*, 5712.
(41) Albright, T. A.; Freeman, W. J.; Schweizer, E. E. *J. Org. Chem.* **1975**, *40*, 3437.
(42) Arney, D. S. J.; Burns, C. J. *J. Am. Chem. Soc.* **1993**, *115*, 9840.
(43) Cantat, T.; Graves, C. R.; Scott, B. L.; Kiplinger, J. L. *Angew. Chem., Int. Ed.* **2009**, *48*, 3681.
(44) The reaction of complex **11b** with elemental sulfur at room temperature immediately afforded $SP\textit{n}\text{-}Bu_3$ as the only phosphorus-containing product.
(45) *International Tables for Crystallography, Vol. C*, 3rd. ed.; Prince, E., Ed.; Springer: 2004.

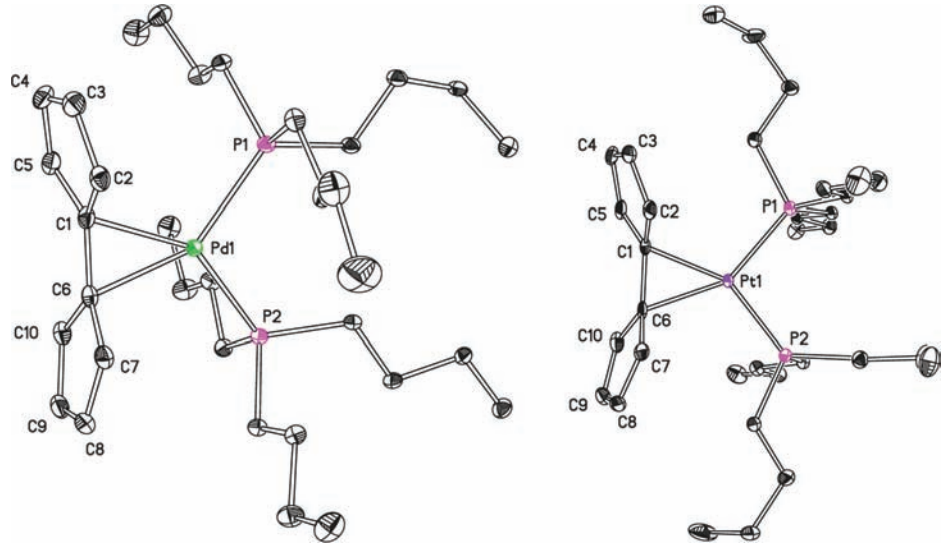

Figure 7. Molecular structures of compounds **11b** (left) and **11c** (right) with thermal ellipsoids at the 30% probability level. Selected bond lengths (Å) and angles (deg): **11b** Pd(1)−C(1), 2.151(2); Pd(1)−C(6), 2.171(2); Pd(1)−P(1), 2.3127(6); Pd(1)−P(2), 2.3162(6); C(1)−C(2), 1.449(3); C(2)−C(3), 1.361(3); C(3)−C(4), 1.435(4); C(4)−C(5), 1.364(3); C(5)−C(1), 1.455(3); C(1)−C(6), 1.440(3); C(6)−C(7), 1.459(3); C(7)−C(8), 1.359(3); C(8)−C(9), 1.433(3); C(9)−C(10), 1.366(3); C(10)−C(6), 1.455(3); P(1)−Pd(1)−P(2), 107.98(2); C(2)−C(1)−C(6), 126.1(2); C(1)−C(6)−C(7), 125.3(2); **11c** Pt(1)−C(1), 2.152(3); Pt(1)−C(6), 2.161(3); Pt(1)−P(1), 2.2586(7); Pt(1)−P(2), 2.2682(8); C(1)−C(2), 1.454(4); C(2)−C(3), 1.371(4); C(3)−C(4), 1.426(5); C(4)−C(5), 1.365(4); C(5)−C(1), 1.452(4); C(1)−C(6), 1.472(4); C(6)−C(7), 1.447(4); C(7)−C(8), 1.356(4); C(8)−C(9), 1.427(5); C(9)−C(10), 1.355(5); C(10)−C(6), 1.458(4); P(1)−Pt(1)−P(2), 99.86(3); C(2)−C(1)−C(6), 125.8(3); C(1)−C(6)−C(7), 123.8(3).

Å] and the sum of angles around these atoms (358.1° and 358.15° for C1 and C6, respectively) suggest the η^2-coordination and partial reduction of the C═C bond. All these data are consistent with the ligation of a neutral [5,5′]bicyclopentadienylidene ligand, formed by the transfer of two electrons from the original carbon-based ligands to each of the sulfur and palladium centers. An analysis of the structure of **11c** resulted in similar conclusions, and further support for the Pt(0)-olefin formulation was provided spectroscopically by the large value observed for the platinum−phosphorus NMR coupling constant (3913 Hz).[46] Important metrical parameters for this compound are also included in Figure 7.

The reaction of the nickela[1]ferrocenophane **4a** with a stoichiometric amount of elemental sulfur was also attempted. The product, however, proved to be more reactive toward S_8 than the Pd- and Pt-[5,5′]bicyclopentadienylidene complexes, and rapidly evolved to SP*n*-Bu_3. Mixing **4a** with an excess of sulfur atoms (1.3 equiv) at −78 °C afforded the same initial complex, which could then be isolated as dark violet needles in moderate yield (27%). It is interesting to note that the NMR spectra of the resulting nickel complex presented some differences compared to those of **11b** and **11c**. Whereas the ^{1}H NMR spectrum of the platinum derivative showed two multiplets for all the [5,5′]bicyclopentadienylidene protons (δ 6.7 and 6.8 ppm), which overlapped in the case of the palladium complex (δ 6.8 ppm), the same spectrum of the nickel complex displays two different sets of signals corresponding to two different cyclopentadiene environments (δ 7.1, 6.9 and 5.9, 4.8 ppm). This suggests that the oxidative coupling of the cyclopentadienyl ligands again occurs but in this instance the [5,5′]bicyclopentadienylidene ligand is η^4:η^0 coordinated to Ni (**11a**, Scheme 5).

Compound **11a** crystallizes in the monoclinic space group $P2_1/c$, and the molecular structure along with important metrical parameters is displayed in Figure 8. The nickel center forms closer contacts to C3 and C4 than to C2 and C5 [2.082(2), 2.054(2), 2.228(2), and 2.154(2) Å, respectively], which are all significantly shorter than the distance to C1 [2.342(2) Å]. These data suggest that the carbon-based ligand is coordinated in an η^4- rather than η^5-fashion and this is consistent with the observed

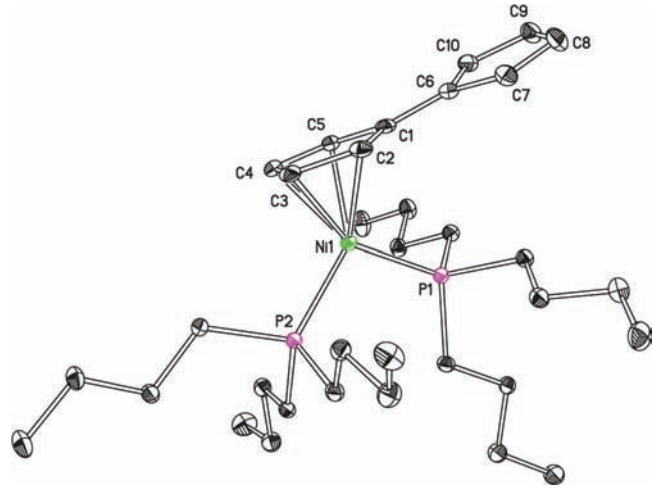

Figure 8. Molecular structure of complex **11a** with thermal ellipsoids at the 30% probability level. Ni(1)−C(1), 2.234(2); Ni(1)−C(2), 2.228(2); Ni(1)−C(3), 2.082(2); Ni(1)−C(4), 2.054(2); Ni(1)−C(5), 2.154(2); Ni(1)−P(1), 2.1754(7); Ni(1)−P(2), 2.1900(7); C(1)−C(2), 1.430(4); C(2)−C(3), 1.396(4); C(3)−C(4), 1.441(4); C(4)−C(5), 1.400(4); C(5)−C(1), 1.464(4); C(1)−C(6), 1.416(3); C(6)−C(7), 1.431(4); C(7)−C(8), 1.378(4); C(8)−C(9), 1.423(4); C(9)−C(10), 1.380(4); C(10)−C(6), 1.436(4); P(1)−Ni(1)−P(2), 106.10(3); C(2)−C(1)−C(6), 126.8(2); C(1)−C(6)−C(7), 125.1(2).

Scheme 5. Reaction of Complex **4a** with Elemental Sulfur

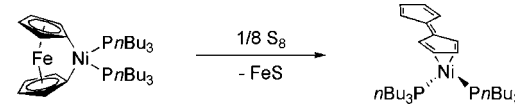

4a **11a**

(46) For recent examples of platinum−phosphorus NMR coupling constants for η^2-olefin complexes, see: Asaro, F.; Lenarda, M.; Pellizer, G.; Storaro, L. *Spectrochim. Acta, Part A* **2000**, *56*, 2167.

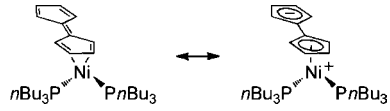

Figure 9. Resonance forms contributing to the bonding in **11a**.

diamagnetic NMR spectrum for a nickel(0) complex. The tetrahedral geometry thus expected for the complex is also in keeping with the observed P1−Ni1−P2 bond angle of 106.10(2)°. The lengths of the C═C bonds coordinated to nickel [1.396(4) and 1.400(4) for C2−C3 and C4−C5, respectively] are longer than those for C7−C8 and C9−C10 [1.378(4) and 1.380(4) Å, respectively], albeit only at the 2σ level of confidence. These latter bond lengths are also markedly longer than that predicted by theory for [5,5′]bicyclopentadienylidene (1.360 Å), as is the exocyclic C═C double bond [1.416(3) Å for C1−C6 *cf.* 1.368 Å].[47b] Conversely, the C−C single bond lengths determined for the pendent ring [1.431(4), 1.436(4), and 1.423(4) Å for C6−C7, C10−C6, and C8−C9, respectively] are all significantly shorter than those calculated. A geometrically similar [5,5′]bicyclopentadienylidene ligand was also observed in the molecular structure of $[\{\eta^4{:}\eta^0\text{-}C_5H_4(C_5H_4)\}Ru(CO)(PMe_3)_2]$,[48b] where such averaging of the carbon−carbon bond lengths was attributed to a significant resonance contribution from a zwitterionic form. Further support for this bonding situation was provided by the ^{13}C NMR spectrum, which exhibited resonances for the pendent ring that were shielded with respect to those measured for [5,5′]bicyclopentadienylidene.[49b] This phenomenon was also observed in the ^{13}C NMR spectrum of $[\{\eta^4{:}\eta^0\text{-}C_5H_4(C_5H_4)\}Mo(CO)_2(PMe_3)_2]$,[48a,c] and the range of chemical shifts observed (δ 110.5−133.7 ppm) is similar to that found for **11a** (δ 116.6−136.4 ppm). The bonding here, therefore, would appear to be best described by the resonance forms displayed in Figure 9.

It is noteworthy that [5,5′]bicyclopentadienylidene itself is unstable with respect to the [2 + 2] cycloaddition product above −30 °C,[49] and that **11b** and **11c**, to the best of our knowledge, represent the first examples of such a molecule being stabilized by η^2-coordination to a metal. Most of the research based on this C_{10}-scaffold has focused on the development of homo- and heterobimetallic $\eta^5{:}\eta^5$-bonded complexes.[50] The syntheses of these compounds, however, have generally proceeded via dihydro[5,5′]bicyclopentadienylidene or the doubly reduced dianion ($[C_{10}H_8]^{2-}$), rather than [5,5′]bicyclopentadienylidene itself.[51] Furthermore, the formation of such a framework from the oxidative coupling of two η^5-bound Cp ligands, as observed for **11a**−**c**, has not previously been reported.

The liberation of SP*n*-Bu_3 during the formation of the [5,5′]bicyclopentadienylidene complexes leads to a decrease of the final yield in which the latter are obtained. Accordingly, the reaction of the Ni complex **4a** with sulfur, by which the [5,5′]bicyclopentadienylidene complex **11a** was obtained in moderate yield, gives rise to the largest amount of $SPBu_3$ (**11a**/$SPBu_3$ of 2:1). This suggests that **11a** exhibits much higher reactivity toward S_8 than **11b**−**c**. Although the decomposition of **11a** and **11b** to give, in part, $SPBu_3$ could be hindered by carrying out the reactions at low temperature it could not be avoided completely. In an attempt to circumvent this problem, we investigated the reaction of the pallada[1]ferrocenophane **4b** with iodine. Monitoring the reaction by $^{31}P\{^1H\}$ NMR spectroscopy showed that although treatment of **4b** with an equimolar amount of iodine at low temperature afforded the Pd-[5,5′]bicyclopentadienylidene complex **11b**, another product (δ 0.7) was also obtained in a *ca.* 1:1 ratio. Addition of an excess of iodine to the reaction mixture caused complete conversion of **11b** into the new product, which was identified by mass spectroscopy as $[PdI_2(Pn\text{-}Bu_3)_2]$.

As mentioned above, the reaction of complexes **4a**−**c** with ferrocenium tetrafluoroborate did not afford the [5,5′]bicyclopentadienylidene complexes. Therefore, it seems likely that the precipitation of binary iron(II) salts from the reaction mixture provides the thermodynamic driving force. [5,5′]Bicyclopentadienylidene can be obtained by a sequence of reactions involving coupling of two cyclopentadienyl anions upon treatment with I_2, double deprotonation of the dihydro[5,5′]bicyclopentadienylidene thus obtained, and subsequent oxidation with O_2.[49b] In order to investigate whether the oxidative coupling of the cyclopentadienyl ligands is a feature common to all metallocenophanes, we attempted the oxidation of dimethylsila[1]ferrocenophane. Treatment of **1** ($ER_x = SiMe_2$) with elemental sulfur, however, did not afford a reaction under the same conditions that proved successful for the group 10 metal derivatives. This result provides further evidence for the transmission of the electronic properties of the late transition metal to the ferrocene moiety, which is reflected in the higher ease of oxidation of the latter compared to that of the sila[1]ferrocenophane.

The low oxidation potentials of **4a**−**c** suggest ready oxidation by sulfur. The HOMO of the molecules is outward pointing and a possible site of attack. Formation of the [5,5′]bicyclopentadienylidene complex may be modeled by removing the Fe atom from **4a**−**c**. In each case optimizing the geometry of the Fe depleted complex proceeded smoothly to an η^2 coordinated metal [5,5′]bicyclopentadienylidene complex, $[M(PH_3)_2(C_{10}H_8)]$ [M = Ni (**12a**), Pd (**12b**), and Pt (**12c**)] (Figure 10a). Structural details are given in the Supporting Information. Given the different coordination geometry for **12a** the energetics of different coordination modes were explored for all three metals. For Ni we were able to identify the η^4 coordination mode as a local minimum (Figure 10b): the two coordination modes were effectively equal in energy (the η^2 mode was more stable by 0.04 eV). For **12b** or **12c** attempts to optimize an η^4 mode with the metal bound to a ring resulted in the metal bound in an η^2

(47) (a) Hinchliffe, A.; Soscún Machado, H. J. *Int. J. Mol. Sci.* **2000**, *1*, 39. (b) Kleinpeter, E.; Holzberger, A.; Wacker, P. *J. Org. Chem.* **2008**, *73*, 56.

(48) (a) Boese, R.; Tolman, W. B.; Vollhardt, K. P. C. *Organometallics* **1986**, *5*, 582. (b) Tilset, M.; Vollhardt, K. P. C. *Organometallics* **1985**, *4*, 2230. (c) Tilset, M.; Vollhardt, K. P. C.; Boese, R. *Organometallics* **1994**, *13*, 3146.

(49) (a) Halton, B. *Eur. J. Org. Chem.* **2005**, 3391. (b) Escher, A.; Rutsch, W.; Nenenschwander, M. *Helv. Chim. Acta* **1986**, *69*, 1644.

(50) (a) Ceccon, A.; Santi, S.; Orian, L.; Bisello, A. *Coord. Chem. Rev.* **2004**, *248*, 683. (b) de Azevedo, C. G.; Vollhardt, K. P. C. *Synlett* **2002**, 1019. (c) Nafady, A.; Geiger, W. E. *Organometallics* **2008**, *27*, 5624.

(51) Reaction of low-valent transition-metal complexes with the unstable dihydro[5,5′]bicyclopentadienylidene: (a) Vollhardt, K. P. C.; Weidman, T. W. *Organometallics* **1984**, *3*, 82. (b) Zhu, B.; Miljanić, O. Š.; Vollhardt, K. P. C.; Westa, M. J. *Synthesis* **2005**, 3373. Reductive coupling between halocyclopentadienyl rings: (c) Ashworth, T. V.; Cuenca Agreda, T.; Herdtweck, E.; Herrmann, W. A. *Angew. Chem., Int. Ed. Engl.* **1986**, *25*, 289. (d) Wielstra, Y.; Gambarotta, S.; Spek, A. L.; Smeets, W. J. J. *Organometallics* **1990**, *9*, 2142. (e) González-Maupoey, M.; Rodríguez, G.; Cuenca, T. *J. Organomet. Chem.* **2002**, *645*, 112. Reaction of transition-metal halides with [5,5′]bicyclopentadienylidene dianion: (f) Smart, J. C.; Pinsky, B. L. *J. Am. Chem. Soc.* **1980**, *102*, 1009. (g) Spink, W. C.; Rausch, M. D. *J. Organomet. Chem.* **1986**, *308*, C1. Deprotonation/oxidation of monocyclopentadienyl systems: (h) Herrmann, W. A.; Andrejewski, D.; Herdteck, E. *J. Organomet. Chem.* **1987**, *319*, 183. (i) Connelly, N. G.; Lucy, A. R.; Payne, J. D.; Galas, A. M. R.; Geiger, W. E. *J. Chem. Soc., Dalton Trans.* **1983**, 1879.

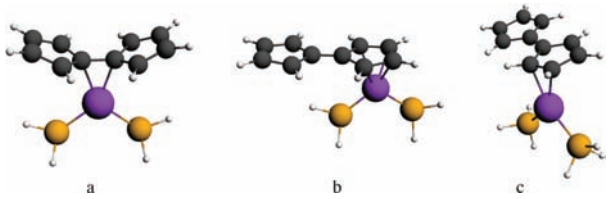

Figure 10. Alternative structures found for $[M(PH_3)_2(C_{10}H_8)]$ (**12a**−**c**).

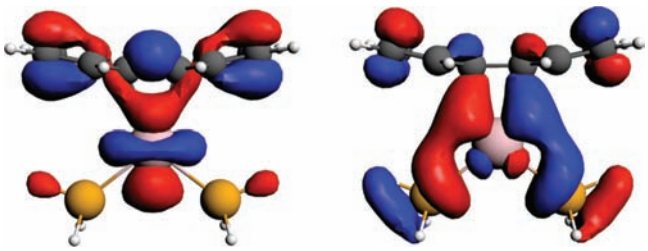

Figure 11. Iso-surfaces for **12c** showing MOs principally involved in Pt[5,5′]bicyclopentadienylidene bonding.

mode to C1 and C2 of the ring (Figure 10c). Again there was negligible energetic difference between the two modes with the coordination to the two bridging C atoms being marginally more stable (Pd by 0.02 eV; Pt by 0.08 eV).

The η^2 preference found for Pd and Pt is consistent with the preference for 16-electron complexes for these two metals. The principal bonding metal bonding orbitals for **12c** are shown in Figure 11.

3. Summary

The complete series of group 10 metalla[1]ferrocenophanes **4a**, **4b**, and **4c** has been synthesized by reaction of the corresponding $[MCl_2(P\textit{n}\text{-}Bu_3)_2]$ [M = Ni (**6a**), Pd (**6b**), and Pt (**6c**)] with dilithioferrocene·tmeda (**5**). Similar to other [1]ferrocenophanes, these species possess highly strained structures, with ring-tilt angles in the range of 24°−28°. A novel feature is the presence of a distorted square planar late transition metal center in the bridge. However, their reactivity displays interesting and in some cases unprecedented features, which contrasts with those characteristic of metallocenophanes that do not contain a square-planar late transition metal complex in the bridge. Although attempts to induce ROP have been unsuccessful to date due to ligand dissociation, the nickel and palladium derivatives **4a** and **4b** react with excess phenyllithium to afford the corresponding stoichiometrically ring-opened species **8a** and **8b**, respectively; apparently chain propagation is not favored, and this prevents polymer formation. Complexes **4a**−**c** are, however, highly reactive toward even weak acids such as alcohols, thiols, or amines, leading to the protonolysis of both of the metal−Cp σ-bonds. Carbon monoxide reacts at the Pd center of **4b** to afford acyl complex **10** upon migratory insertion. Under the same conditions, however, **4a** extrudes $[Ni(CO)_2(P\textit{n}\text{-}Bu_3)_2]$ and **4c** is unreactive. In contrast with other strained ferrocenophanes, species **4a**−**c** are inherently electron rich relative to ferrocene based on cyclic voltammetry experiments. These metalla[1]ferrocenophanes react with oxidants such as oxygen and elemental sulfur affording the [5,5′]bicyclopentadienylidene (pentafulvalene) complexes **11a**−**c**, of which **11b** and **11c** constitute the first examples of η^2-complexes containing a neutral [5,5′]bicyclopentadienylidene ligand. These reactions are proposed to proceed through oxidative cleavage of the iron−cyclopentadienyl bonds followed by carbon−carbon bond formation upon coupling of the cyclopentadienide units.

The results herein described provide new insight into how the nature of the transannular bridge influences not only the structural features of the [1]ferrocenophane and the strain present but also the electronic properties and reactivity of these complexes. Further work in our group will target a range of related strained metal-bridged metallocenophanes, particularly those with more robust ancillary ligation, which will offer the prospect of access to stable metallopolymers using ROP procedures.

4. Computational Methods

Quantum chemical calculations were performed using density functional methods of the Amsterdam Density Functional (Version ADF2008.01) package.[52−54] TZP basis sets were used with triple-ξ accuracy sets of Slater-type orbitals, with polarization functions added to all atoms. Relativistic corrections were made using the ZORA (zero-order relativistic approximation) formalism for Pd and Pt,[55−59] and the core electrons were frozen up to 1s for C, 2p for P, Fe and Ni 3d for Pd and 4d for Pt. The local density approximation of Vosko, Wilk, and Nusair[60] was utilized together with the nonlocal exchange correction by Becke[61,62] and nonlocal correlation corrections by Perdew.[63] All quoted electronic structure data from optimized structures use an integration grid of 5.0 and were verified as minima using frequency calculations. For some compounds low imaginary frequencies were found corresponding to rotation of PH_3 groups, a barrierless process. Topological analyses of the electron density were performed using the XAIM program.[64] The *adf2aim* executable, which is provided with the standard source code of the ADF program, was used to convert the tape21 file to a wave function (.wfn) file. XAIM was then used to locate and characterize the critical points.

Acknowledgment. I. Matas would like to thank the Fundación Ramón Areces for a postdoctoral fellowship. I. Manners thanks the EPSRC for financial support, the E.U. for a Marie Curie Chair, and the Royal Society for a Wolfson Research Merit Award. Johnson Matthey are gratefully acknowledged for the loan of precious metal salts.

Supporting Information Available: Experimental procedures, crystallographic methods, and data and computational data. This material is available free of charge via the Internet at http://pubs.acs.org.

JA103367E

(52) Fonseca Guerra, C.; Snijder, J. G.; Te Velde, G.; Baerends, E. J. *Theor. Chem. Acc.* **1998**, *99*, 391.
(53) Te Velde, G.; Bickelhaupt, F. M.; Baerends, E. J.; Fonseca Guerra, C.; Van Gisbergen, S. J. A.; Snijders, J. G.; Ziegler, T. *J. Comput. Chem.* **2001**, *22*, 931.
(54) ADF2008.01, SCM, Theoretical Chemistry, Vrije Universiteit, Amsterdam, The Netherlands, http://www.scm.com.
(55) Vanlenthe, E.; Baerends, E. J.; Snijders, J. G. *J. Chem. Phys.* **1993**, *99*, 4597.
(56) Vanlenthe, E.; Baerends, E. J.; Snijders, J. G. *J. Chem. Phys.* **1994**, *101*, 9783.
(57) Vanlenthe, E.; Baerends, E. J.; Snijders, J. G. *J. Chem. Phys.* **1996**, *105*, 6505.
(58) Vanlenthe, E.; Ehlers, A.; Baerends, E. J. *J. Chem. Phys.* **1999**, *110*, 8943.
(59) Vanlenthe, E.; VanLeeuwen, R.; Baerends, E. J.; Snijders, J. G. *Int. J. Quantum Chem.* **1996**, *57*, 281.
(60) Vosko, S. H.; Wilk, L.; Nusair, M. *Can. J. Phys.* **1980**, *58*, 1200.
(61) Becke, A. D. *Phys. Rev. A* **1988**, *38*, 3098.
(62) Becke, A. D. *J. Chem. Phys.* **1988**, *88*, 1053.
(63) Perdew, J. P. *Phys. Rev. B* **1986**, *33*, 8800.
(64) Alba, J. C. O.; Jané, C. B. *XAim*; 1998 (Download free of charge from the web distribution site: http://www.quimica.urv.es/XAIM/).